



Article

The Significant Role of PA28 $\alpha\beta$ in CD8⁺ T Cell-Mediated Graft Rejection Contrasts with Its Negligible Impact on the Generation of MHC-I Ligands

Katharina Inholz ^{1,2}, Ulrika Bader ², Sarah Mundt ³ and Michael Basler ^{1,2,*}

¹ Biotechnology Institute Thurgau (BITg) at the University of Konstanz, 8280 Kreuzlingen, Switzerland; katharina.inholz@uni-konstanz.de

² Division of Immunology, Department of Biology, University of Konstanz, 78464 Konstanz, Germany

³ Institute of Experimental Immunology, University of Zurich, 8057 Zurich, Switzerland

* Correspondence: michael.basler@bitg.ch

Abstract: The proteasome generates the majority of peptides presented on MHC class I molecules. The cleavage pattern of the proteasome has been shown to be changed via the proteasome activator (PA)28 alpha beta (PA28 $\alpha\beta$). In particular, several immunogenic peptides have been reported to be PA28 $\alpha\beta$ -dependent. In contrast, we did not observe a major impact of PA28 $\alpha\beta$ on the generation of different major histocompatibility complex (MHC) class I ligands. PA28 $\alpha\beta$ -knockout mice infected with the *lymphocytic choriomeningitis virus* (LCMV) or *vaccinia* virus showed a normal cluster of differentiation (CD) 8 response and viral clearance. However, we observed that the adoptive transfer of wild-type cells into PA28 $\alpha\beta$ -knockout mice led to graft rejection, but not vice versa. Depletion experiments showed that the observed rejection was mediated by CD8⁺ cytotoxic T cells. These data indicate that PA28 $\alpha\beta$ might be involved in the development of the CD8⁺ T cell repertoire in the thymus. Taken together, our data suggest that PA28 $\alpha\beta$ is a crucial factor determining T cell selection and, therefore, impacts graft acceptance.

Keywords: proteasome; PA28 $\alpha\beta$; CD8 T cell response; adoptive cell transfer; rejection; antigen processing; antigen presentation



Citation: Inholz, K.; Bader, U.; Mundt, S.; Basler, M. The Significant Role of PA28 $\alpha\beta$ in CD8⁺ T Cell-Mediated Graft Rejection Contrasts with Its Negligible Impact on the Generation of MHC-I Ligands. *Int. J. Mol. Sci.* **2024**, *25*, 5649. <https://doi.org/10.3390/ijms25115649>

Academic Editor: Efstratios Stratikos

Received: 10 April 2024

Revised: 19 May 2024

Accepted: 20 May 2024

Published: 22 May 2024



Copyright: © 2024 by the authors. Licensee MDPI, Basel, Switzerland. This article is an open access article distributed under the terms and conditions of the Creative Commons Attribution (CC BY) license (<https://creativecommons.org/licenses/by/4.0/>).

1. Introduction

The ubiquitin–proteasome system is the main producer of peptides presented on MHC class I molecules. The differently expressed catalytic active subunits in the standard proteasome ($\beta 1$, $\beta 2$ and $\beta 5$), the immunoproteasome ($\beta 1i$, $\beta 2i$ and $\beta 5i$) and the thymoproteasome ($\beta 1i$, $\beta 2i$ and $\beta 5t$) lead to an altered MHC-I peptide repertoire in different tissues [1–7]. In addition, the binding of different regulatory particles to the core 20S proteasome shapes the peptide repertoire [8,9]. The most common bound activator is the 19S regulator, which drastically increases the catalytic activity of the 20S proteasome and forms the 26S proteasome by binding to the 20S core particle. Additionally, there are other activators able to bind to the 20S core particle, for example, the proteasome activator 28 alpha beta (PA28 $\alpha\beta$). In contrast to the 19S activator, PA28 $\alpha\beta$ can shape the peptide generation of its substrates in an ATP independent process [10]. PA28 $\alpha\beta$ is composed of three alpha and four beta subunits, forming a ring-like structure [11]. It can bind at both sides of the proteasome or build a hybrid proteasome together with one 19S regulator [12,13]. This hybrid proteasome has been shown to hydrolyze the substrate into rather short and hydrophilic peptides at a faster rate than the 26S proteasome. Interestingly, although PA28 $\alpha\beta$ was discovered to strongly activate the hydrolysis of short fluorogenic peptide substrates by the 20S proteasome, the protein turnover of PA28 $\alpha\beta$ bound to the 20S proteasome alone was shown to be as slow as for the 20S proteasome [14]. Although there are several hypotheses how PA28 $\alpha\beta$ shapes and changes peptide production, the underlying mechanisms are not fully

understood. PA28 $\alpha\beta$ might serve as a sieve, leading to a longer stay of peptides within the 20S proteasome and, therefore, favoring the production of short peptides [15]. Alternatively, it has been discussed that by binding of PA28 $\alpha\beta$ to the 20S proteasome, the catalytic activity of the 20S subunits might be changed [14].

Both subunits of PA28 $\alpha\beta$ are induced by the inflammatory cytokine interferon (IFN)- γ . Due to this, and the fact that it can bind to both the immunoproteasome as well as the standard proteasome with the same affinity, a role of PA28 $\alpha\beta$ in immunological processes has been proposed [15,16]. Indeed, an impact of PA28 $\alpha\beta$ on the generation of *murine cytomegalovirus* (MCMV), *coxsackievirus B3* and *influenza A virus* pathogen-derived peptides has been reported [17–19]. However, the biological relevance in immunity seems rather low because PA28 $\alpha\beta$ -knockout cells in mice showed a mild impact of PA28 $\alpha\beta$ on the generation of immunogenic peptides [20,21].

Although the vast majority of peptides produced by PA28 $\alpha\beta$ -capped proteasomes bound to the proteasome are too small for efficient MHC class I presentation [14], a role for PA28 $\alpha\beta$ in the generation of self-peptides has been proposed [22]. The proteasome seems to play a pivotal role in the selection of cytotoxic T cells in the thymus [1,2,23–26]. The unique thymoproteasome shapes the peptide repertoire, which is presented in cortical thymic epithelial cells (cTECs) for the positive selection of CD4⁺CD8⁺ thymocytes [27,28]. Subsequent to the positive selection, the remaining T cells undergo negative selection, which is based on the presentation of peptides mostly generated by the immunoproteasome and expressed by medullary thymic epithelial cells (mTECs) and dendritic cells (DCs). PA28 $\alpha\beta$ is expressed in the thymus [26] and, therefore, has the possibility to bind to the thymoproteasome or the immunoproteasome, contributing to the peptide repertoire for T cell selection. However, if proteasome activators such as PA28 $\alpha\beta$ indeed contribute to the selection of T cells in the thymus in addition to shaping the peptide repertoire presented in the periphery remains to be investigated.

In this study, we re-investigated the contribution of PA28 $\alpha\beta$ to MHC-I antigen processing and viral infection in vivo in PA28 $\alpha\beta$ -deficient mice.

2. Results

2.1. PA28 $\alpha\beta$ Does Not Influence the Distribution of Immune-Cell Subsets or the MHC Class I Expression in Naïve Mice

To determine if PA28 $\alpha\beta$ could influence the composition of immune cells in the spleen and thymus, PA28 $\alpha\beta$ -deficient mice and C57BL/6 control mice were stained for CD4, CD8, CD3, CD19, NK1.1, CD11b and CD11c and analyzed by flow cytometry. The assessment of these immune-cell population did not reveal any impact attributable to the absence of PA28 $\alpha\beta$ (Figure 1a,b). Given the important role of the proteasome in the MHC class I presentation of immunogenic peptides, we investigated the potential impact of PA28 $\alpha\beta$ on the MHC class I surface expression. Murine embryonic fibroblasts (MEFs) derived from either wild-type mice or PA28 $\alpha\beta$ -deficient mice were treated with IFN- γ . The H-2K^b surface expression was analyzed by flow cytometry. IFN- γ induced an upregulation of H-2K^b in a time-dependent manner. However, the MHC class I surface expression remained unchanged in the absence of PA28 $\alpha\beta$ (Figure 1c). Comparative analyses of the most prevalent immune-cell subsets in the spleen between wild-type and PA28 $\alpha\beta$ -knockout mice revealed no significant differences in the MHC class I surface expression on T cells (CD3⁺), cytotoxic T cells (CD8⁺), T helper cells (CD4⁺), B cells (CD19⁺) or natural killer cells (NK1.1⁺) (Figure 1d). Our findings suggest that the potential contribution of PA28 $\alpha\beta$ to the processing of immunogenic peptides is rather negligible.

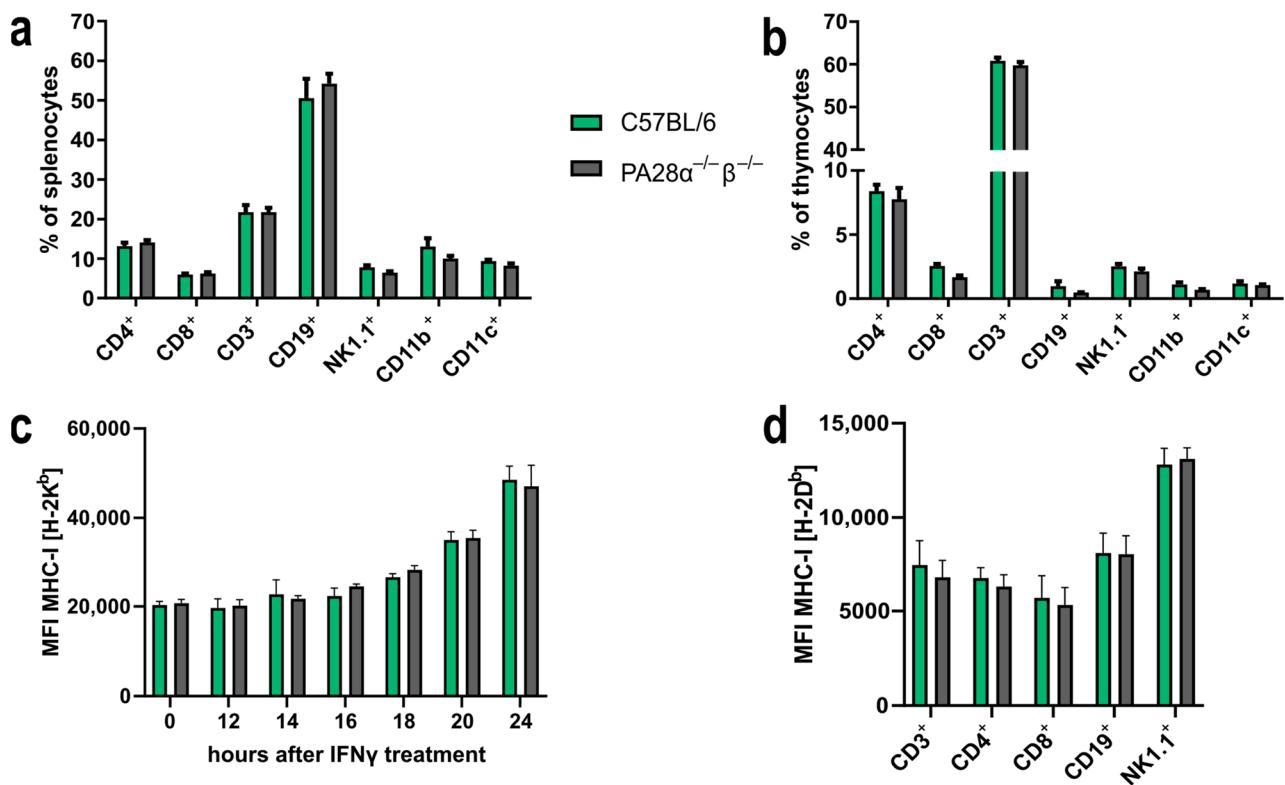


Figure 1. PA28αβ expression alters neither the distribution of immune-cell subsets in the spleen and thymus nor the MHC class I expression of surface on MEFs or splenocytes. (a,b) Percentage of indicated immune-cell subsets in the spleen (a) or thymus (b) was measured by flow cytometry from naïve wild-type or PA28αβ-knockout mice ($n = 5$ mice per group, measured in duplicate). (c) Median fluorescence intensity (MFI) of surface MHC class I H-2K^b expression of MEF populations from either PA28αβ-knockout or wild-type mice measured by flow cytometry after IFN-γ treatment for the indicated time points. Data show two independent MEF populations per wild-type and knockout measured as duplicates in two independent experiments. (d) MFI of surface expression of MHC class I H-2D^b measured by flow cytometry on indicated immune-cell populations in the spleen of wild-type or PA28αβ-knockout mice ($n = 5$ mice per group, measured in duplicate). (a–d) Wild-type mice are represented by green bars and PA28αβ-knockout mice are represented by grey bars. Data are shown as mean ± SEM, statistically analyzed using the Student's *t*-test. Unless otherwise specified, the analyses revealed no statistically significant differences.

2.2. Presentation of Several Tested Immunogenic MHC Class I Peptides Remains Unaltered by PA28αβ Expression

It has been described that PA28αβ increases the MHC class I presentation of some immunogenic peptides [18,29,30], whereas others remain unaffected [21,31]. To address if PA28αβ affected further T cell epitopes, five different H-2D^b/K^b-restricted LCMV-derived epitopes were investigated. MEFs from either wild-type or PA28αβ-knockout mice were infected with LCMV-WE and the amount of peptides presented on MHC class I molecules was detected using peptide-specific CTL lines against glycoprotein (GP) or nucleoprotein (NP) NP_{396–404}/Db, GP_{276–286}/Db, GP_{33–41}/Db, GP_{118–125}/Kb and NP_{205–212}/Kb. Similar to the LCMV-derived NP_{118–126}/Ld epitope [30], PA28αβ had no significant effect on the presentation of different LCMV-derived peptides (Figure 2a–e). Externally, peptide-loaded MEFs were used as positive controls (Supplementary Figure S1a–e).

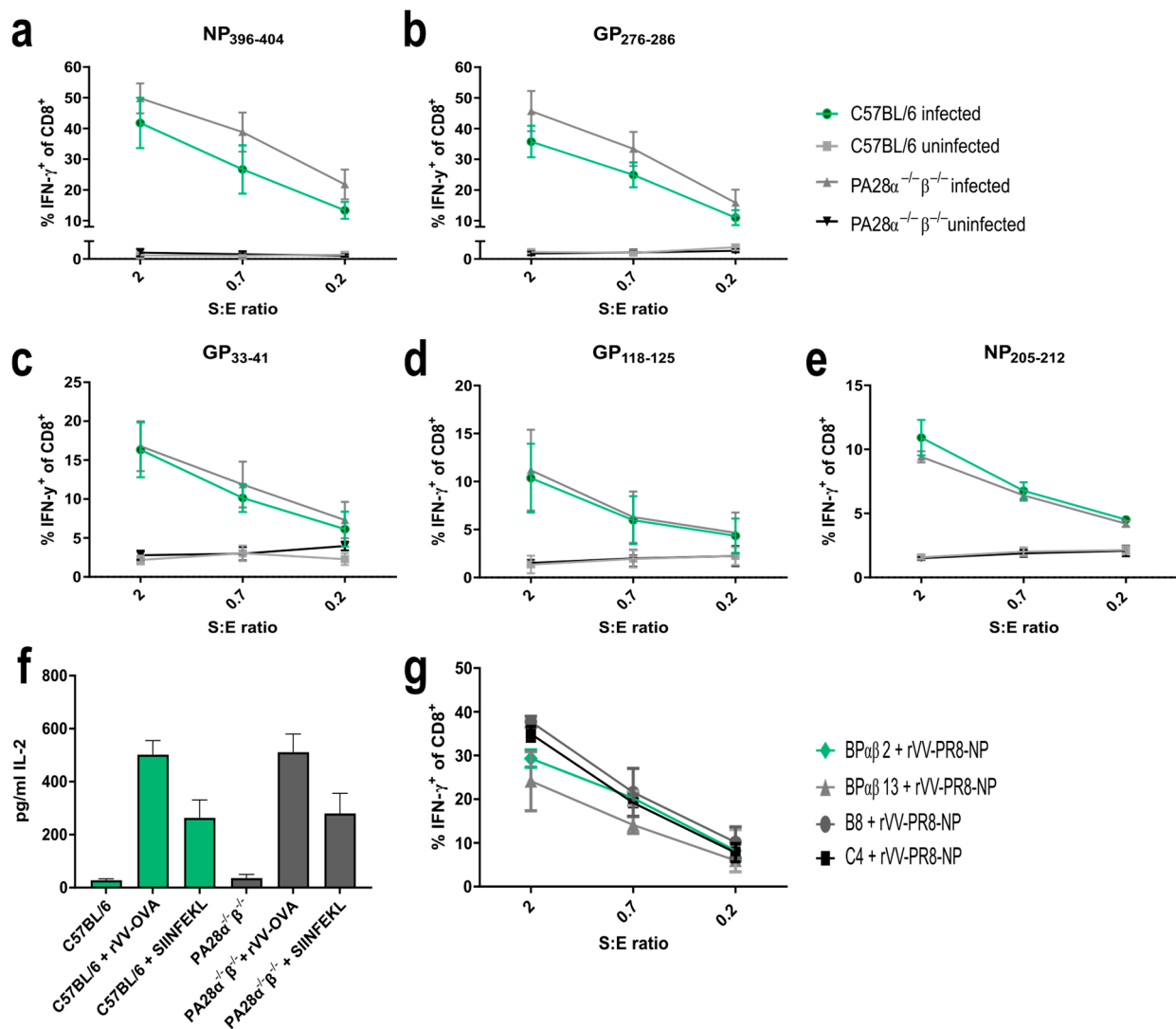


Figure 2. Expression of PA28 $\alpha\beta$ does not change the presentation of several LCMV-derived MHC-I peptides, SIINFEKL or Influenza-NP₁₄₇₋₁₅₅. (a–e) IFN- γ -stimulated MEFs (48 h) from three individual preparations of C57BL/6 or two individual preparations of PA28 α ^{-/-}β^{-/-} mice were LCMV-WE-infected for 24 h and afterwards co-cultured with indicated peptide-specific CTL lines at different S:E ratios (stimulators: MEFs; effector: CTL). Activation of CTL lines was analyzed by staining for CD8 and intracellular IFN- γ after five hours of co-culture. Shown are the percentages of IFN- γ -positive cells of CD8⁺ cells as determined by flow cytometry for 3–5 independent experiments per peptide. (f) MEFs from C57BL/6 or PA28 α ^{-/-}β^{-/-} mice were infected with rVV-OVA for 3 h and SIINFEKL presentation was analyzed using B3Z T cell hybridoma. IL-2 secretion was measured by ELISA. Externally, SIINFEKL peptide-loaded MEFs (indicated as SIINFEKL) were used as positive controls ($n =$ three independent experiments). Wild-type mice are represented by green bars and PA28 $\alpha\beta$ -knockout mice are represented by grey bars. (g) The parental cell lines C4 and B8 (low PA28 $\alpha\beta$ expression) and the cell lines BP $\alpha\beta$ 13 and BP $\alpha\beta$ 2 (high PA28 $\alpha\beta$ expression) were infected with rVV-PR8 for 3 h and co-cultured with a NP₁₄₇₋₁₅₅-specific CTL line. After 4.5 h of co-culture, activation of CTL lines was analyzed by staining for CD8 and intracellular IFN- γ . Shown are the percentages of IFN- γ -positive cells of CD8⁺ cells as determined by flow cytometry. (a–g) Data are shown as mean \pm SEM, statistically analyzed using the Student's t -test or by a two-way ANOVA using Tukey's multiple comparisons test. Unless otherwise specified, the analyses revealed no statistically significant differences.

Next, we investigated the presentation of ovalbumin-derived SIINFEKL. rVV-Ova-infected MEFs from wild-type or PA28 $\alpha^{-/-}\beta^{-/-}$ mice were infected with recombinant *vaccinia* viruses expressing ovalbumin (rVV-OVA). The SIINFEKL presentation was determined using SIINFEKL-specific B3Z T cell hybridoma activation. The peptide presentation was independent of PA28 $\alpha\beta$, confirming previous results (Figure 2f) [20]. Furthermore, the presentation of *influenza*-derived NP₁₄₇₋₁₅₅/Ld was shown to depend on PA28 $\alpha\beta$ [29]. To re-investigate the presentation of this peptide, PA28 $\alpha\beta$ -overexpressing cell lines (BP $\alpha\beta$ m2 and BP $\alpha\beta$ 13) and their parental cell lines C4 and B8 were infected with a *vaccinia* virus expressing *influenza*-NP (rVV-PR8-NP). The amount of NP₁₄₇₋₁₅₅ peptides presented on MHC class I molecules was detected using peptide-specific CTL lines (Figure 2g). No difference in NP₁₄₇₋₁₅₅ presentation between cells overexpressing PA28 $\alpha\beta$ (BP $\alpha\beta$ 2 and BP $\alpha\beta$ 13) and cells with low PA28 $\alpha\beta$ (C4 and B8) could be detected. Taken together, our data investigating 7 different MHC-I peptides suggest a rather negligible impact of PA28 $\alpha\beta$ on the generation and presentation of immunogenic peptides.

2.3. Immune Response after Vaccinia or LCMV Infection Is Not Altered in PA28 $\alpha^{-/-}\beta^{-/-}$ Mice

The peptide presentation on MHC-I is a crucial step in the induction of a cytotoxic T cell response. Here, we used a *vaccinia* or an LCMV-WE infection model system to address whether PA28 $\alpha\beta$ influenced the presentation *in vivo*, thereby altering the induction of a cytotoxic T cell response. Wild-type or PA28 $\alpha\beta$ -deficient mice were infected with VV-WR and viral titers were determined in the ovaries on day 6 post-infection. *Vaccinia*-infected PA28 $\alpha\beta$ -knockout mice did not show altered viral titers in the ovaries 6 days after infection compared with infected wild-type mice (Figure 3a). An analysis of the cytotoxic T cell response on day 8 post-infection to four different *vaccinia*-derived peptides did not reveal any differences (Figure 3b). Next, wild-type or PA28 $\alpha\beta$ -deficient mice were infected with LCMV-WE. Viral titers were determined in the spleen on day 2, 4, 6 and 8 post-infection (Figure 3c). Similar viral titers were observed in wild-type and PA28 $\alpha\beta$ -deficient mice. The viral clearance in LCMV-infected C57BL/6 mice was strictly dependent on cytotoxic T cells [32]. Mice lacking PA28 $\alpha\beta$ were able to eliminate LCMV within 8 days, indicating that these mice were fully competent in mounting a cytotoxic T cell response. Indeed, the CTL response in PA28 $\alpha\beta$ -knockout mice and wild-type mice directed against GP₃₃₋₄₁/Db/Kb, NP₃₉₆₋₄₀₄/Db, GP₂₇₆₋₂₈₆/Db, GP₉₂₋₁₀₁/Db, GP₁₁₈₋₁₂₅/Kb and NP₂₀₅₋₂₁₂/Kb on day 8 post-LCMV-WE infection by intracellular cytokine staining (ICS) for IFN- γ showed a similar strength and hierarchy (Figure 3d). Our results, derived from two different viral infection models, were in agreement with a rather mild impact of PA28 $\alpha\beta$ on the induction of CD8⁺ T cells after *Listeria monocytogenes* infection in mice [20].

The *in vivo* CTL response (Figure 3) was in line with the *in vitro* antigen-presentation assays (Figure 2) as both datasets showed that PA28 $\alpha\beta$ had no impact on the presentation of the investigated MHC-I ligands.

2.4. Thymocyte Development and TCR Subsets Remain Unaltered by PA28 $\alpha\beta$ Deficiency

As PA28 $\alpha\beta$ is expressed in the thymus [26] and because the proteasome plays an important role in the selection of CD8⁺ T cells, we investigated whether PA28 $\alpha\beta$ influenced the development of T cells in the thymus. We checked the CD44⁺/CD25⁺ expression, which is used to differentiate between CD4⁻/CD8⁻ double-negative (DN) 1, DN2, DN3 and DN4 thymocyte populations. No discernible differences were observed in the DN development between wild-type and PA28 $\alpha\beta$ -knockout mice (Figure 4a). Additionally, the CD5 expression, serving as a marker for the intensity of T cell receptor (TCR) interactions with self-MHC peptides, and the CD69 expression, indicating the successful positive selection of T cells, were evaluated across CD4⁺ single positive (SP), CD8⁺ SP, and double-positive (DP) thymocytes in both wild-type and PA28 $\alpha\beta$ -deficient mice. The expression levels of CD5 and CD69 on all examined subsets did not vary, which indicated an unimpeded T cell development in PA28 $\alpha\beta$ -deficient mice (Figure 4b). Furthermore, the TCR composition was examined using a flow cytometry TCR V β screening panel for both CD8⁺ splenocytes and

CD8⁺ thymocytes from wild-type and PA28 $\alpha\beta$ -deficient mice (Figures 4c,d and S2 for CD4⁺ splenocytes and CD4⁺ thymocytes). The TCR V β analysis revealed no differences in either the bulk T cell selection in the thymus or in the periphery in the spleen of PA28 $\alpha\beta$ -deficient mice. In addition, the H-2D^b and H-2K^b surface expression on mTECs and cTECs was analyzed in the thymus of wild-type mice and PA28 $\alpha\beta$ -deficient mice (Supplementary Figure S3). Neither the total amount of mTECs or cTECs nor their MHC-I surface expression were different in PA28 $\alpha\beta$ -deficient mice.

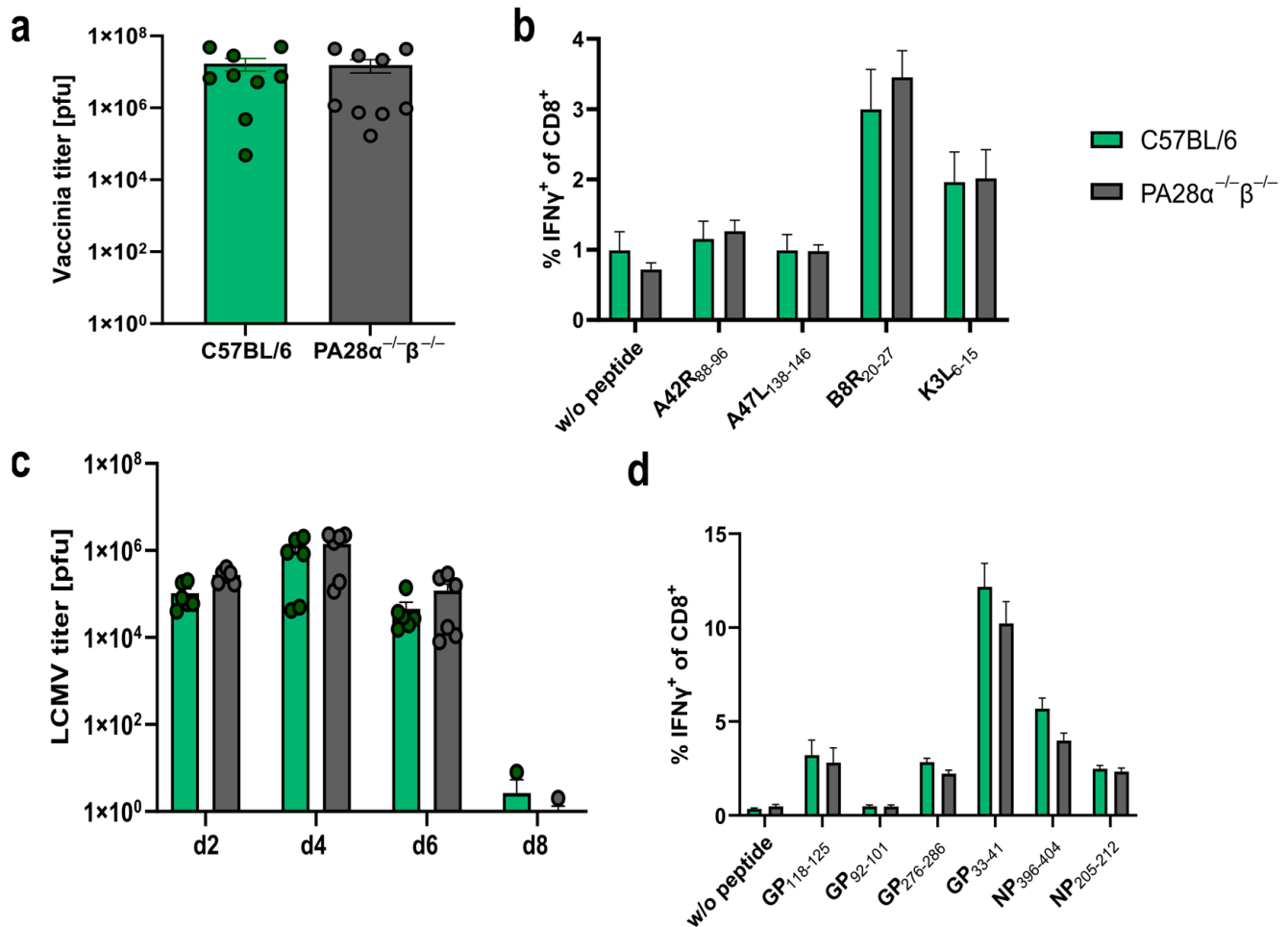


Figure 3. *Vaccinia* and *LCMV* titers as well as the cytotoxic T lymphocyte (CTL) response are not altered in PA28 $\alpha\beta$ -knockout mice. (a–d) Wild-type and PA28 $\alpha\beta$ -knockout mice were infected with VV-WR (a,b) or *LCMV*-WE (c,d). (a) Viral titers analyzed in ovaries on day 6 post VV-WR infection ($n = 9$ mice per group, represented by green dots for wild-type mice and grey dots for PA28 $\alpha\beta$ -knockout mice). (b,d) Eight days post-infection, spleen cells were harvested and stimulated *in vitro* with the indicated *vaccinia* virus- (b) or *LCMV*-derived (d) peptides for 5 h, and analyzed by flow cytometry after staining for CD8 and intracellular IFN- γ . Unstimulated cells (indicated by w/o peptide) were used as a negative control ($n = 9$ mice per group). (c) Viral titers analyzed in the spleen on indicated days post-*LCMV*-WE infection ($n = 3$ –6 mice per group, represented by green dots for wild-type mice and grey dots for PA28 $\alpha\beta$ -knockout mice). (a–d) Wild-type mice are represented by green bars and PA28 $\alpha\beta$ -knockout mice by grey bars. Data are shown as mean \pm SEM, statistically analyzed using the Student's *t*-test. Unless otherwise specified, the analyses revealed no statistically significant differences.

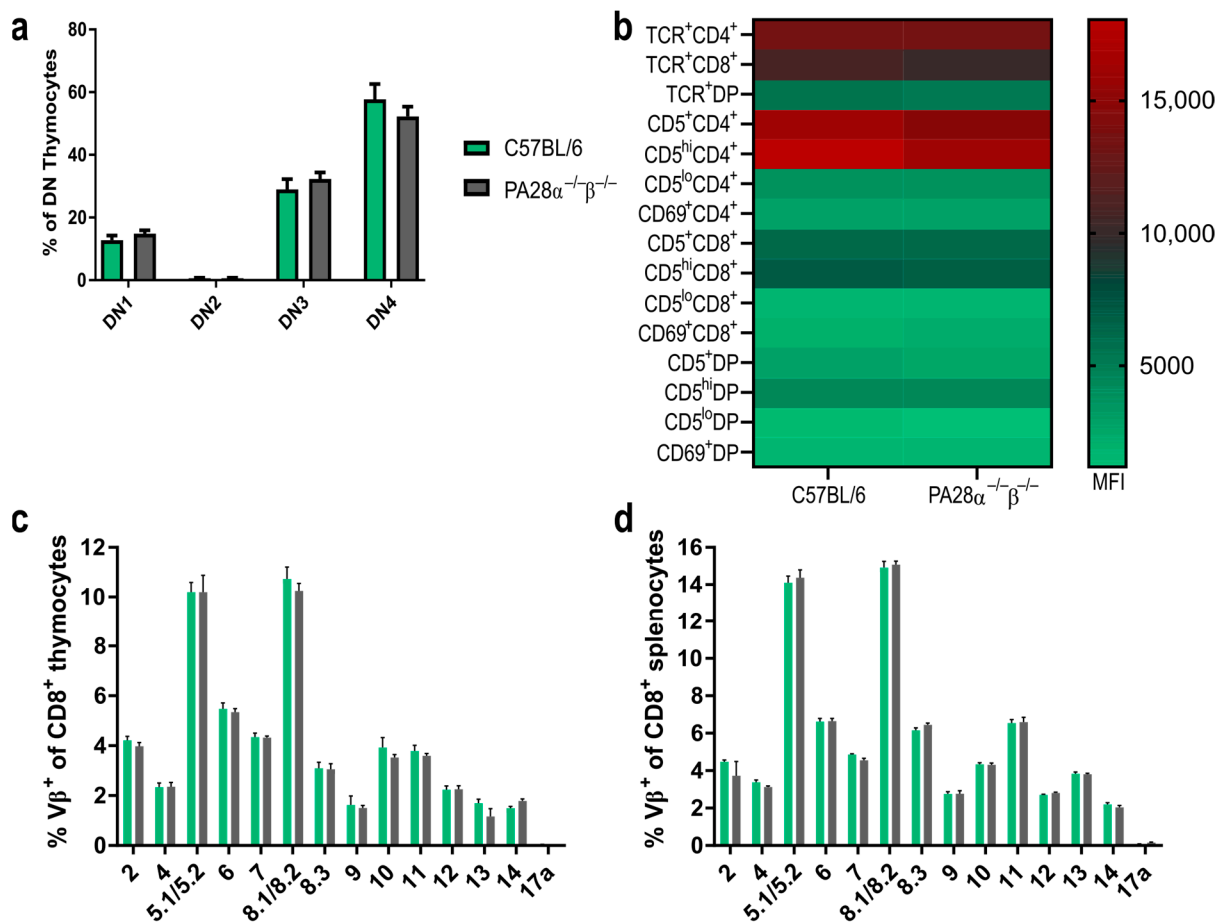


Figure 4. Thymocyte development and TCR distribution is not altered in the absence of PA28 $\alpha\beta$. (a) DN (CD4⁻/CD8⁻) populations in the thymus of wild-type mice or PA28 $\alpha\beta$ -deficient mice were investigated according to their CD44 and CD25 expression. DN1: CD44⁺CD25⁻; DN2: CD44⁺CD25⁺; DN3: CD44^{-/lo}CD25⁺; DN4: CD44^{-/lo}CD25⁻ ($n = 10$ mice per group). (b) Median fluorescence intensity (MFI) of TCR, CD5 or CD69 on CD4 SP (CD4⁺/CD8⁻) (indicated as CD4⁺), CD8 SP (CD4⁻/CD8⁺) (indicated as CD8⁺) and DP (CD4⁺/CD8⁺) (indicated as DP) thymocytes was measured for $n = 10$ mice per group of wild-type or PA28 $\alpha\beta$ -deficient mice. (c,d) Flow cytometric analysis of indicated V β variable segments of TCRs from CD8 SP thymocytes (c) or splenocytes. Wild-type mice are represented by green bars and PA28 $\alpha\beta$ -knockout mice are represented by grey bars. (d) Derived from C57BL/6 mice or PA28 $\alpha\beta$ -deficient mice ($n = 5$ mice per group). V β 17a was not expressed in the C57BL/6 background and was used as a negative control. (a–d) Data are shown as mean \pm SEM, statistically analyzed using the Student's t -test. Unless otherwise specified, the analyses revealed no statistically significant differences.

2.5. PA28 $\alpha\beta$ -Deficient Mice Reject Transplanted Wild-Type Cells in a CD8⁺ T Cell-Dependent Manner

The proteasome is an attractive target and a crucial factor determining transplantation efficiency [33–36]. Hence, it seems obvious that PA28 $\alpha\beta$, as a regulator of the proteasome, might influence transplantation efficiency. Therefore, we performed adoptive cell transfer experiments. Magnetically sorted wild-type CD3⁺ CD45.1⁺ T cells were transferred into PA28 $\alpha\beta$ -knockout mice (expressing the CD45.2 isoform) and vice versa. In weekly assessments, the survival of the transferred T cells was analyzed in the blood by flow cytometry (Figure 5a–d). We observed a rejection of wild-type cells in PA28 $\alpha\beta$ -knockout mice, while transferred wild-type cells remained stable in wild-type mice over five weeks. An analysis of the spleen after five weeks post-transfer showed that wild-type T cells were completely

rejected (Figure 5b). Interestingly, wild-type mice receiving T cells from PA28 $\alpha\beta$ -knockout mice did not reject the transferred cells (Figure 5c,d).

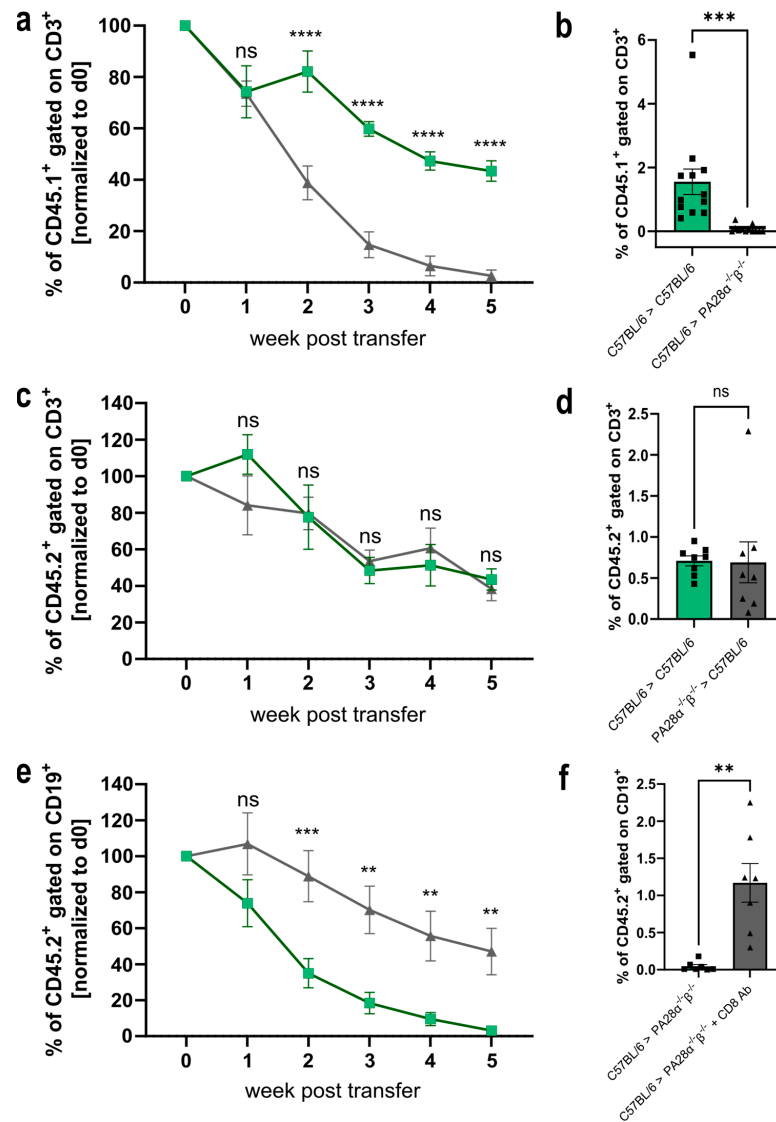


Figure 5. Wild-type cells are rejected in PA28 $\alpha\beta$ -knockout mice in a CD8⁺ T cell-dependent manner. (a,c) Magnetically sorted CD3⁺ T cells from wild-type (CD45.1⁺) or PA28 $\alpha\beta$ -knockout mice (CD45.2⁺) were transferred into PA28 $\alpha\beta$ -knockout or wild-type mice. The rejection of the transferred cells was monitored in the blood weekly. Green lines indicate the transfer of wild-type cells into wild-type mice, while grey lines show the transfer of wild-type cells into PA28 $\alpha\beta$ deficient mice (a) or PA28 $\alpha\beta$ deficient cells into wild-type mice (c). (b,d) Five weeks after the transfer, the percentage of CD45.1⁺ or CD45.2⁺, respectively, was measured in the spleen. (e) MACS-sorted CD19⁺ B cells were transferred into PA28 $\alpha\beta$ -knockout mice, which were either treated weekly with an anti-CD8⁺-depleting antibody (indicated as CD8 Ab) or left untreated. Rejection of the transferred cells was monitored in the blood weekly. Green lines indicate the transfer of wild-type cells into PA28 $\alpha\beta$ deficient mice, while grey line indicate the transfer of PA28 $\alpha\beta$ deficient cells into wild-type mice treated with an CD8 Ab. (f) Five weeks after the transfer, the percentage of CD45.2⁺ was measured in the spleen ($n = 7-12$ mice per group). (a–f) Cell transfers between mice of the same gender were performed. The transfer of cells between donors and recipients of different genders is shown in Supplementary Figure S4. (b,d,f) Recipient wild-type mice are represented by green bars and recipient PA28 $\alpha\beta$ -knockout mice are represented by grey bars. Data statistically analyzed using a two-way ANOVA with Tukey’s multiple comparisons test. ** $p < 0.01$; *** $p < 0.001$; **** $p < 0.0001$. ns: Not significant.

To gain insight into the underlying mechanism of the rejection of wild-type T cells transferred to PA28 $\alpha\beta$ -knockout mice, we depleted the CD8⁺ T cells (Supplementary Figure S4) in the PA28 $\alpha\beta$ -knockout host mice before and during the transfer of wild-type CD19⁺ B cells. To avoid the antibody-mediated depletion of transferred T cells in the host mice, we used magnetically sorted CD19⁺ B cells for the transfer experiments. Similar to T cells (Figure 5a,b) wild-type B cells were rejected in PA28 $\alpha\beta$ -deficient recipient mice. Interestingly, transferred wild-type B cells were not rejected in CD8 T cell-depleted host mice. These data show that the rejection of wild-type cells in PA28 $\alpha\beta$ -deficient mice is mediated by cytotoxic T cells.

Consequently, the decreased survival of adoptively transferred wild-type cells into PA28 $\alpha\beta$ -deficient mice prompted us to investigate the influence of PA28 $\alpha\beta$ in vivo using a murine skin transplantation model.

For this purpose, C57BL/6 or PA28 $\alpha^{-/-}\beta^{-/-}$ tail-skin grafts were transplanted onto the back of PA28 $\alpha\beta$ -deficient mice or wild-type mice, respectively. Skin transplantation from wild-type mice to wild-type mice was used as a negative control. The graft on the recipient mice was monitored daily for signs of rejection. Both the wild-type and PA28 $\alpha\beta$ -deficient mice did not show any signs of graft rejection within 11 weeks (Supplementary Figure S5). These data show that PA28 $\alpha\beta$ had no influence on skin transplantation in the used model. It has been reported that immunoproteasome-deficient mice might harbor an altered T cell repertoire [2,23–26]. Furthermore, the ubiquitin-like modifier FAT10, which targets proteins for proteasomal degradation, has been shown to modify the T cell repertoire [37]. Hence, as the proteasome regulator PA28 $\alpha\beta$ is also expressed in the thymus [26], an altered T cell repertoire in PA28 $\alpha\beta$ -deficient mice might be responsible for the rejection of transferred wild-type cells in PA28 $\alpha\beta$ -deficient mice (Figure 5). To investigate if the PA28 $\alpha\beta$ expression altered the T cell repertoire in the thymus, thereby being responsible for the rejection of transferred wild-type cells, we decided to use bone-marrow chimeras. Wild-type or PA28 $\alpha\beta$ -deficient mice were irradiated and reconstituted with either wild-type or PA28 $\alpha\beta$ -deficient bone marrow. We intended to transfer magnetically purified cells 8 weeks post-reconstitution in a similar experiment as performed in Figure 5. If wild-type cells transferred to PA28 $\alpha\beta$ -deficient mice reconstituted with wild-type bone marrow were still rejected, then PA28 $\alpha\beta$ was required in radioresistant cells—most likely, thymic epithelial cells. However, within two weeks post-radiation, most of the PA28 $\alpha\beta$ -deficient mice reconstituted with wild-type bone marrow had to be euthanized due to severe health conditions. As the PA28 $\alpha\beta$ mice reconstituted with PA28 $\alpha\beta$ bone marrow were healthy, the PA28 $\alpha\beta$ -deficient mice were not susceptible to radiation per se. Although these data further strengthen the conclusion that the PA28 $\alpha\beta$ expression is an important parameter in transplantation, additional experiments need to be performed to elucidate the underlying mechanisms of the rejection of wild-type bone marrow in PA28 $\alpha\beta$ -deficient mice.

3. Discussion

In the present study, we re-investigated the role of PA28 $\alpha\beta$ in the generation of MHC class I peptides and furthermore investigated its role in viral infections and its impact on tissue grafting.

The fact that PA28 $\alpha\beta$ is IFN- γ -inducible and binds to the proteasome led to the hypothesis that PA28 $\alpha\beta$ was involved in MHC class I antigen processing. Peptide generation studies have proposed that the binding of PA28 $\alpha\beta$ to the proteasome leads to the release of smaller and more hydrophilic peptides [14]. Different in vitro and in vivo studies have shown an impact of PA28 $\alpha\beta$ on the generation of some MHC-I ligands [31,38]. Furthermore, it has been shown that in PA28 $\alpha\beta$ -deficient cells, the IFN- γ -inducible MHC class I expression was reduced, which indicates an impact of PA28 $\alpha\beta$ on the presentation of ligands upon IFN- γ stimulation [39]. Yet, the biological relevance remains unclear. In contrast to these studies, we investigated several MHC-I ligands using in vitro antigen-presentation assays and could not confirm a major impact of PA28 $\alpha\beta$ on the generation of immunogenic MHC-I peptides (Figure 2). Additionally, we did not observe a difference in MHC-I

upregulation in IFN- γ -stimulated wild-type and PA28 $\alpha\beta$ -deficient MEFs (Figure 1c). In agreement, we did not observe an impact of PA28 $\alpha\beta$ on the induction of a cytotoxic T cell response in two different viral models in vivo. This was in line with initial findings that PA28 $\alpha\beta$ -knockout mice did not show a difference in body-weight loss and mortality after *influenza* infection [31]. Furthermore, Sijts et al. showed a negligible role of PA28 $\alpha\beta$ in the *Listeria monocytogenes*-specific CD8 and CD4 response eight days after infection [20]. In line with these results, we showed that PA28 $\alpha\beta$ has no crucial role in the antiviral response after LCMV or *vaccinia* virus infections. No difference in the cytotoxic T cell response and viral titers was observed (Figure 3). Interestingly, there are indications that in COVID-19 patients, SARS-CoV-2 infection can trigger PA28 $\alpha\beta$ upregulation [40]. Whether this upregulation is just a result of increased IFN- γ or whether PA28 $\alpha\beta$ has additional beneficial effects on the infection outcome itself remain to be investigated.

Our results from adoptive cell transfer experiments suggest a role of PA28 $\alpha\beta$ in the generation of self-peptides. PA28 $\alpha\beta$ expression in the thymus indicates that by binding to the thymoproteasome in cTECs, it can shape the generation of peptides responsible for the positive selection of CD8⁺ cells [26]. Additionally, the DCs, mTECs and stromal cells responsible for negative selection in the thymus express immunoproteasomes, which are capable of binding to PA28 $\alpha\beta$. This indicates that PA28 $\alpha\beta$ might be involved in the generation of the peptides responsible for negative selection in the thymus [3,26]. We could not detect any differences between the abundance of mTECs and cTECs or any differences in the surface expression of MHC class I peptides on mTECs and cTECs when comparing wild-type and PA28 $\alpha\beta$ -knockout mice (Supplementary Figure S3). This strengthens the hypothesis that the observed rejection of wild-type cells in knockout mice relies on the role of PA28 $\alpha\beta$ in shaping the peptide repertoire present in the TECs rather than a bulk MHC-I expression.

Thus, the absence of PA28 $\alpha\beta$ in the thymus may lead to an altered MHC-I peptidome, positively and negatively selecting cells in the thymus compared with wild-type cells. The selection processes in the presence of new or missing self-peptides in PA28 $\alpha\beta$ -deficient mice can lead to an altered T cell repertoire. This might result in the observed depletion of transferred wild-type cells in knockout mice as some peptides presented on wild-type MHC class I are recognized as foreign peptides. This notion is strongly supported by the fact that cytotoxic T cells were responsible for the rejection of transferred cells in our model (Figure 5c). The production of low-affinity peptides for MHC class I presentation is crucial for positive selection by cTECs. The ability of PA28 $\alpha\beta$ to shape a peptide repertoire that is too short for an efficient MHC presentation might have an impact on the positive selection of T cells by increasing the pool of low-affinity self-peptides [14]. Thus, a lack of PA28 $\alpha\beta$ could result in an altered TCR diversity. Furthermore, a PA28 $\alpha\beta$ deficiency in mTECs and DCs in the thymus might lead to missing self-peptides, which are required for the negative selection of cytotoxic T cells. This is important in the context of transplantation as T cells leave the thymus able to trigger an allo-response after transplantation when organs or cells from a healthy donor are transplanted. A potential change in T cell clonality, which might trigger rejection after the transfer of cells, was not observed in our flow cytometry studies on thymocyte development, TCR usage and TCR subsets in PA28 $\alpha\beta$ -knockout mice. This implies that PA28 $\alpha\beta$ does not alter the bulk MHC-I presentation in the thymus, but that differences are probably related to a few peptides. To detect these subtle differences, an analysis of the TCR subsets with more sensitive methods such as TCR sequencing might reveal PA28 $\alpha\beta$ -induced alterations in the T cell repertoire. The clonal expansion of a few T cells after transplantation is sufficient for a graft rejection. These clones display only a small proportion compared with the bulk T cells and might easily remain undetected by flow cytometry V β screening (Figure 4) [41].

Investigating the tissue-specific peptidome in allo-recognition has been shown to be highly important to identify self-peptides impacting graft survival [42]. To further elaborate the involvement of PA28 $\alpha\beta$ in graft rejection, we performed tail-skin transplantation experiments. We observed no rejection of skin transferred from wild-type mice onto

PA28 $\alpha\beta$ -knockout mice (Supplementary Figure S5). Interestingly, skin transferred from wild-type mice onto LMP7 $^{-/-}$ mice was rejected within 2 to 6 weeks in earlier studies [33], indicating that the immunoproteasome, compared with PA28 $\alpha\beta$ in the thymus, has a broader effect on MHC-I ligand processing and, thus, the T cell repertoire. The 26S and the PA28 $\alpha\beta$ hybrid proteasomes interact with different proteins [9,43]; therefore, some MHC-I ligands can be over-represented, leading to recognition by and rejection of specific cytotoxic T cells. Such peptides might be differently expressed on transferred immune cells compared with transplanted skin. Furthermore, the PA28 $\alpha\beta$ expression in transferred immune cells and skin might be different. As the transplanted skin needs to undergo vascularization, which takes several days to weeks, an acute rejection is less common in this model and might be responsible for the difference in the rejection of skin and transferred cells [44]. The possibility that peptides originating from PA28 $\alpha\beta$ itself were present in the cells of wild-type mice cannot be excluded. Nevertheless, as PA28 $\alpha\beta$ is expressed in the skin, we would have expected a rejection in the skin transplantation model, which we did not observe. The rejection of transferred cells but not skin is, therefore, based on the impact of PA28 $\alpha\beta$ on peptide generation rather than being present itself on MHC.

Our attempt at using bone-marrow chimeras to corroborate that selection processes in the thymus were the underlying mechanism for the rejection of transferred immune cells failed due to the immediate rejection of the wild-type bone marrow in the PA28 $\alpha\beta$ -knockout mice. Despite not being able to investigate the impact of PA28 $\alpha\beta$ -dependent thymic selection processes in bone-marrow chimeras, this outcome further highlighted the importance of PA28 $\alpha\beta$ in graft acceptance. As proteasomal activators have a major impact on the catalytic activity of the proteasome, they must be taken into consideration before and after transplantations [45].

We concluded that the role of PA28 $\alpha\beta$ in the generation of immunogenic MHC-I ligands has been overestimated. Putative alterations in MHC-I processing had no biological relevance in our two viral infection models. PA28 $\alpha\beta$ was not required to conduct a potent immune response after viral infections and eliminate the viruses. Strikingly, PA28 $\alpha\beta$ was found to be an essential factor in graft acceptance.

4. Materials and Methods

4.1. Cell Lines

Mouse embryonal fibroblasts derived from either C57BL/6 or PA28 $\alpha^{-/-}\beta^{-/-}$ were produced as described previously and maintained in a DMEM medium (Gibco, Fisher Scientific, Schwerte, Germany) supplemented with 10% FCS (Gibco, Fisher Scientific, Schwerte, Germany) and 100 U/mL penicillin/100 μ g/mL streptomycin (Gibco, Fisher Scientific, Schwerte, Germany) [46]. The cell lines C4 [30], B8 [47], BP $\alpha\beta$ 13 and BP $\alpha\beta$ 2 [30] and the hybridoma cell line B3Z [48] were maintained in IMDM (Gibco, Fisher Scientific, Schwerte, Germany) supplemented with 10% FCS and 100 U/mL penicillin/100 μ g/mL streptomycin. BSC-40 and MC57 cell lines were cultured in MEM (Gibco, Fisher Scientific, Schwerte, Germany) supplemented with 5% FCS and 100 U/mL penicillin/100 μ g/mL streptomycin. Adherent cells were detached by incubation with 0.05% trypsin-EDTA (Gibco, Fisher Scientific, Schwerte, Germany) for 5 min at 37 °C. All cell lines were maintained at 37 °C with 5% CO₂ in a humidified atmosphere.

4.2. Mice and Ethical Statement

C57BL/6 (H-2b) and B6.SJL-PtprcaPep3b/BoyJ (Ly5.1 congenic mice) mice were originally purchased from Charles River, Sulzfeld, Germany. PA28 $\alpha^{-/-}\beta^{-/-}$ mice (B6.Cg-Psme1/Psme2tm1Tchi) were kindly provided by T. Chiba (Department of Molecular Oncology, Tokyo Metropolitan Institute of Medical Science, Tokyo, Japan) [31]. All animals were bred in air-conditioned rooms with a controlled temperature of 21 °C, 55% relative humidity and constant ventilation (17 air changes/h) in the animal facility of the University of Konstanz under pathogen-free conditions with a 12 h light/dark cycle. Animals were provided ad libitum access to a standard animal diet and water. For the infection models,

the mice were infected either with 200 pfu LCMV-WE i.v. or with 2×10^6 pfu VV-WR i.p. for the indicated time points. The animal experiments were approved by the Review Board of Governmental Presidium Freiburg (G-20/071, G-23/023, G-23/027, I-18/03 and I-22/001).

4.3. Antigen-Specific CTL Lines

CTL lines were generated as previously described [2]. In brief, C57BL/6 mice and PA28 $\alpha^{-/-}$ $\beta^{-/-}$ mice were either infected with 200 pfu LCMV-WE i.v. or with 2×10^6 pfu recombinant *vaccinia* i.p. (rVV-PR8-NP) viruses. Four weeks after infection, single-cell suspensions of splenocytes were incubated with 40 U/mL IL-2 and incubated with 10^{-5} M of the corresponding peptide for 8 days. IL-2 was freshly added every second day. Dead cells were removed after 8 days via Ficoll-PaqueTM (Merck, Darmstadt, Germany) gradient centrifugation. Viable cells were incubated with the corresponding peptide and IL-2 for another 7–10 days. A second Ficoll-PaqueTM gradient was performed one day prior to the experiment.

4.4. Antigen-Presentation Assay and Hybridoma Assay

For the LCMV antigen-presentation assays, C57BL/6 and PA28 $\alpha^{-/-}$ $\beta^{-/-}$ MEFs were stimulated with 100 U/mL IFN- γ for 48 h. Afterwards, cells were infected with LCMV-WE (MOI 0.5) for 24 h at 37 °C. Viable peptide-specific CTLs were incubated with MEFs for 5 h with the addition of 10 μ g/mL Brefeldin A (Thermo Fisher Scientific, Darmstadt, Germany). Antigen presentation was analyzed via intracellular staining for the IFN- γ^+ of CD8⁺ CTLs. For the SIINFEKL presentation, C57BL/6 and PA28 $\alpha^{-/-}$ $\beta^{-/-}$ MEFs were stimulated with 100 U/mL IFN- γ for 48 h followed by three hours of infection with rVV-Ova (MOI 10). Next, 5×10^5 MEFs were co-cultured with 10^6 B3Z hybridomas for 24 h at 37 °C. The activation of hybridomas was analyzed via an IL-2 ELISA according to the manufacturer's protocol (mouse IL-2 ELISA Ready-SET-Go![®], eBiosciences, Frankfurt a. Main, Germany). For influenza A peptide generation (NP₁₄₇₋₁₅₅), C4, B8, BP $\alpha\beta$ 13 and BP $\alpha\beta$ 2 were infected with rVV-PR8-NP₁₄₇₋₁₅₅ (MOI 10) for 4.5 h. Subsequently, the infected cells were co-cultured with peptide-specific CTLs for three hours. Antigen presentation was analyzed via the intracellular staining of IFN- γ^+ CD8⁺ CTLs as previously described [25].

4.5. mTEC and cTEC Preparation

Thymi of three to four week old mice were cut into small pieces and digested with 0.25 mg/mL collagenase D (Roche, Mannheim, Germany), 1 U/mL dispase I (Gibco, Fisher Scientific, Schwerte, Germany) and 25 μ g/mL DNase I (Roche, Mannheim, Germany) in RPMI supplemented with 2% FCS and 25 mM HEPES at 37 °C using a gentleMACS (C Tubes, Miltenyi, Miltenyi Biotec GmbH, Bergisch Gladbach, Germany, Program 37_ABDK_1). Single-cell suspensions were stained for the flow cytometry analysis.

4.6. Flow Cytometry

Single-cell suspensions from the spleen and thymus or MEFs were labeled with fluorochrome-conjugated antibodies in a FACS buffer (2% FCS, 2 mM EDTA and 2 mM NaN₃ in 1x PBS) for 20 min at 4 °C. For intracellular staining, cells were fixed with 4% paraformaldehyde and permeabilized using a FACS buffer containing 0.1% saponin (Quilaja sp., Sigma-Aldrich, Darmstadt, Germany). Flow cytometry was performed using a BD FACSLyricTM instrument (BD Biosciences, Heidelberg, Germany). The following antibodies were purchased from the indicated companies and used in the indicated concentrations: CD3 ϵ -APC (145-2C11, BioLegend, Koblenz, Germany; 1:250), CD4-APC (GK1.5, eBioscienceTM, Frankfurt a. Main, Germany; 1:250), CD4-PE (GK1.5, BioLegend, Koblenz, Germany; 1:250), CD4-BV510 (GK1.5, BioLegend, Koblenz, Germany; 1:250), CD5-PE (53-7.3, BD PharmingenTM, Heidelberg, Germany; 1:250), CD8a-APC (53-6.7, BioLegend, Koblenz, Germany; 1:250), CD8a-PE (53-6.7, BioLegend, Koblenz, Germany; 1:250), CD11b-FITC (M1/70, eBioscienceTM, Frankfurt a. Main, Germany; 1:250), CD11b-PE (M1/70,

eBioscience™, Frankfurt a. Main, Germany; 1:250), CD19-FITC (eBio1D3, eBioscience™, Frankfurt a. Main, Germany; 1:250), CD25-PECy7 (3C7, BioLegend, Koblenz, Germany; 1:250), CD44-APC Fire Cy750 (IM7, BioLegend; 1:250), CD45.1-APC (A20, Miltenyi Biotec GmbH, Bergisch Gladbach, Germany; 1:40), CD45-BV421 (30-F11, BioLegend, Koblenz, Germany; 1:250), CD45.2-PE (104-2, Miltenyi Biotec GmbH, Bergisch Gladbach, Germany; 1:40), CD69-BV421 (H1.2F3, BioLegend, Koblenz, Germany; 1:250), B220-PerCP (RA3-6B2, BD Pharmingen™, Heidelberg, Germany; 1:250), IFN- γ -FITC (XMG1.2, BioLegend, Koblenz, Germany; 1:150), NK1.1-PE (PK136, BD Pharmingen™, Heidelberg, Germany; 1:250), EpCAM-APC (G8.8, eBioscience™, Frankfurt a. Main, Germany; 1:250), Ly-51-FITC (6C3, BD Pharmingen™, Heidelberg, Germany; 1:250) and TCR V β Screening Panel (BD Pharmingen™, Heidelberg, Germany; concentration as indicated in the protocol).

4.7. Adoptive Cell Transfer

CD3⁺ cells were purified using a CD3 ϵ MicroBead Kit (Miltenyi Biotec GmbH, Bergisch Gladbach, Germany) and CD19⁺ using a Pan B Cell Isolation Kit II (Miltenyi Biotec GmbH, Bergisch Gladbach, Germany) according to the manufacturer's protocols. Next, 1×10^7 cells in 100 μ L PBS were injected i.v. Blood was taken once a week for five weeks and analyzed for CD3⁺ or CD19⁺ cells, respectively. CD8 depletion was performed by an i.p. injection of a CD8 α -depleting antibody (250 μ g, purified from clone YTS 169.4.2) once a week, starting one day prior to the adoptive cell transfer. The depletion efficiency was checked via flow cytometry. The cell transfer of cells from male mice into female mice was used as a control for rejection and is depicted in Supplementary Figure S4a.

4.8. Skin Transplantation

Skin transplantation experiments were performed as previously described [49]. Briefly, the skin of the tails of sacrificed donor mice was transplanted onto the back of recipient mice. After bandage removal, graft survival was monitored over five weeks.

4.9. LCMV and Vaccinia Titer Determination

The LCMV titer was titrated on MC57 cells as previously described [50]. The vaccinia titer was titrated on BSC-40 cells. Next, 1.5×10^5 BSC-40 cells were seeded the day before by adding the organ lysates into a 24-well plate. The organ samples were prepared as a ten-fold serial dilution and 200 μ L of the lysate or the dilutions were added to the BSC-40 cells. One hour after the addition of the lysates and dilutions, 1 mL MEM was added and the cells were incubated for 24 h. Afterwards, the medium was aspirated and the plaques were stained with 0.5% (*w/v*) crystal violet for 20 min. The crystal violet was washed away and the plaques were counted and calculated according to the dilution.

4.10. Statistics

The statistical analysis was performed using a two-tailed Student's *t*-test, a one-way or a two-way ANOVA followed by a Bonferroni post hoc or Tukey's test for a comparison of multiple groups. Unless noted differently in the figure legends, data from at least three experiments or $n \geq 3$ were presented as the mean \pm SEM. The statistical analyses were performed using GraphPad Prism software (version 9.5.1, GraphPad Software, Inc., La Jolla, CA, USA).

Supplementary Materials: The following supporting information can be downloaded at: <https://www.mdpi.com/article/10.3390/ijms25115649/s1>.

Author Contributions: K.I. performed the experiments and wrote the manuscript. U.B. performed the experiments. S.M. performed the skin transplantation experiments. M.B. designed and performed the experiments, refined the manuscript and supervised the project. All authors have read and agreed to the published version of the manuscript.

Funding: This work was supported by the "Forschungspreis Walter Enggist" (to M Basler) and German Research Foundation Grant GR 1517/25-1 (to M Basler).

Institutional Review Board Statement: The animal study protocol was approved by the Review Board of Governmental Presidium Freiburg (G-20/071, G-23/023, G-23/027, I-18/03 and I-22/001).

Informed Consent Statement: Not applicable.

Data Availability Statement: The data that support the findings of this study are available from the corresponding author upon reasonable request.

Acknowledgments: We thank the facility for flow cytometry (FlowKon) at the University of Konstanz for their help with flow cytometry and the animal research center (TFA) of the University of Konstanz for mouse breeding. We thank Dennis Horvath for proofreading the manuscript.

Conflicts of Interest: The authors declare no conflicts of interest.

References

1. Watanabe, A.; Yashiroda, H.; Ishihara, S.; Lo, M.; Murata, S. The Molecular Mechanisms Governing the Assembly of the Immuno- and Thymoproteasomes in the Presence of Constitutive Proteasomes. *Cells* **2022**, *11*, 1580. [[CrossRef](#)] [[PubMed](#)]
2. Basler, M.; Mundt, S.; Groettrup, M. The Immunoproteasome Subunit LMP7 Is Required in the Murine Thymus for Filling up a Hole in the T Cell Repertoire. *Eur. J. Immunol.* **2018**, *48*, 419–429. [[CrossRef](#)] [[PubMed](#)]
3. Inholz, K.; Anderl, J.L.; Klawitter, M.; Goebel, H.; Maurits, E.; Kirk, C.J.; Fan, R.A.; Basler, M. Proteasome Composition in Immune Cells Implies Special Immune-Cell-Specific Immunoproteasome Function. *Eur. J. Immunol.* **2024**, *54*, e2350613. [[CrossRef](#)] [[PubMed](#)]
4. Rock, K.L.; York, I.A.; Goldberg, A.L. Post-Proteasomal Antigen Processing for Major Histocompatibility Complex Class I Presentation. *Nat. Immunol.* **2004**, *5*, 670–677. [[CrossRef](#)] [[PubMed](#)]
5. Strehl, B.; Seifert, U.; Krüger, E.; Heink, S.; Kuckelkorn, U.; Kloetzel, P.M. Interferon-Gamma, the Functional Plasticity of the Ubiquitin-Proteasome System, and MHC Class I Antigen Processing. *Immunol. Rev.* **2005**, *207*, 19–30. [[CrossRef](#)]
6. Takahama, Y. The Thymoproteasome in Shaping the CD8+ T-Cell Repertoire. *Curr. Opin. Immunol.* **2023**, *83*, 102336. [[CrossRef](#)] [[PubMed](#)]
7. Basler, M.; Lauer, C.; Moebius, J.; Weber, R.; Przybylski, M.; Kisselev, A.F.; Tsu, C.; Groettrup, M. Why the Structure but Not the Activity of the Immunoproteasome Subunit Low Molecular Mass Polypeptide 2 Rescues Antigen Presentation. *J. Immunol.* **2012**, *189*, 1868–1877. [[CrossRef](#)]
8. Kuckelkorn, U.; Stübler, S.; Textoris-Taube, K.; Kilian, C.; Niewianda, A.; Henklein, P.; Janek, K.; Stumpf, M.P.H.; Mishto, M.; Liepe, J. Proteolytic Dynamics of Human 20S Thymoproteasome. *J. Biol. Chem.* **2019**, *294*, 7740–7754. [[CrossRef](#)] [[PubMed](#)]
9. Shibatani, T.; Carlson, E.J.; Larabee, F.; McCormack, A.L.; Früh, K.; Skach, W.R. Global Organization and Function of Mammalian Cytosolic Proteasome Pools: Implications for PA28 and 19S Regulatory Complexes. *Mol. Biol. Cell* **2006**, *17*, 4962–4971. [[CrossRef](#)]
10. Kasahara, M.; Flajnik, M.F. Origin and Evolution of the Specialized Forms of Proteasomes Involved in Antigen Presentation. *Immunogenetics* **2019**, *71*, 251–261. [[CrossRef](#)]
11. Huber, E.M.; Groll, M. The Mammalian Proteasome Activator PA28 Forms an Asymmetric A4β3 Complex. *Structure* **2017**, *25*, 1473–1480.e3. [[CrossRef](#)] [[PubMed](#)]
12. Cascio, P.; Call, M.; Petre, B.M.; Walz, T.; Goldberg, A.L. Properties of the Hybrid Form of the 26S Proteasome Containing Both 19S and PA28 Complexes. *EMBO J.* **2002**, *21*, 2636–2645. [[CrossRef](#)] [[PubMed](#)]
13. Cascio, P.; Goldberg, A.L. Preparation of Hybrid (19S-20S-PA28) Proteasome Complexes and Analysis of Peptides Generated during Protein Degradation. *Methods Enzymol.* **2005**, *398*, 336–352. [[CrossRef](#)]
14. Raule, M.; Cerruti, F.; Benaroudj, N.; Migotti, R.; Kikuchi, J.; Bachi, A.; Navon, A.; Dittmar, G.; Cascio, P. PA28αβ Reduces Size and Increases Hydrophilicity of 20S Immunoproteasome Peptide Products. *Chem. Biol.* **2014**, *21*, 470–480. [[CrossRef](#)] [[PubMed](#)]
15. Cascio, P. PA28αβ: The Enigmatic Magic Ring of the Proteasome? *Biomolecules* **2014**, *4*, 566–584. [[CrossRef](#)] [[PubMed](#)]
16. Schmidtke, G.; Schregle, R.; Alvarez, G.; Huber, E.M.; Groettrup, M. The 20S Immunoproteasome and Constitutive Proteasome Bind with the Same Affinity to PA28αβ and Equally Degrade FAT10. *Mol. Immunol.* **2017**, *113*, 22–30. [[CrossRef](#)]
17. Sijts, A.; Sun, Y.; Janek, K.; Kral, S.; Paschen, A.; Schadendorf, D.; Kloetzel, P.M. The Role of the Proteasome Activator PA28 in MHC Class I Antigen Processing. *Mol. Immunol.* **2002**, *39*, 165–169. [[CrossRef](#)]
18. Respondek, D.; Voss, M.; Kühlewindt, I.; Klingel, K.; Krüger, E.; Beling, A. PA28 Modulates Antigen Processing and Viral Replication during Coxsackievirus B3 Infection. *PLoS ONE* **2017**, *12*, e0173259. [[CrossRef](#)]
19. Stohwasser, R.; Soza, A.; Eggers, M.; Koszinowski, U.H.; Kloetzel, P.M. PA28αβ Double and PA28β Single Transfectant Mouse B8 Cell Lines Reveal Enhanced Presentation of a Mouse Cytomegalovirus (MCMV) Pp89 MHC Class I Epitope. *Mol. Immunol.* **2000**, *37*, 13–19. [[CrossRef](#)]
20. de Graaf, N.; van Helden, M.J.G.; Textoris-Taube, K.; Chiba, T.; Topham, D.J.; Kloetzel, P.M.; Zaiss, D.M.W.; Sijts, A.J.A.M. PA28 and the Proteasome Immunsubunits Play a Central and Independent Role in the Production of MHC Class I-Binding Peptides in Vivo. *Eur. J. Immunol.* **2011**, *41*, 926–935. [[CrossRef](#)]
21. Schwarz, K.; van den Broek, M.; Kostka, S.; Kraft, R.; Soza, A.; Schmidtke, G.; Kloetzel, P.-M.; Groettrup, M. Overexpression of the Proteasome Subunits LMP2, LMP7, and MECL-1, But Not PA28α/β, Enhances the Presentation of an Immunodominant Lymphocytic Choriomeningitis Virus T Cell Epitope. *J. Immunol.* **2000**, *165*, 768–778. [[CrossRef](#)] [[PubMed](#)]

22. McCarthy, M.K.; Weinberg, J.B. The Immunoproteasome and Viral Infection: A Complex Regulator of Inflammation. *Front. Microbiol.* **2015**, *6*, 21. [[CrossRef](#)]
23. Chen, W.; Norbury, C.C.; Cho, Y.; Yewdell, J.W.; Bennink, J.R. Immunoproteasomes Shape Immunodominance Hierarchies of Antiviral CD8+ T Cells at the Levels of T Cell Repertoire and Presentation of Viral Antigens. *J. Exp. Med.* **2001**, *193*, 1319–1326. [[CrossRef](#)] [[PubMed](#)]
24. Osterloh, P.; Linkemann, K.; Tenzer, S.; Rammensee, H.G.; Radsak, M.P.; Busch, D.H.; Schild, H. Proteasomes Shape the Repertoire of T Cells Participating in Antigen-Specific Immune Responses. *Proc. Natl. Acad. Sci. USA* **2006**, *103*, 5042–5047. [[CrossRef](#)] [[PubMed](#)]
25. Basler, M.; Moebius, J.; Elenich, L.; Groettrup, M.; Monaco, J.J. An Altered T Cell Repertoire in MECL-1-Deficient Mice. *J. Immunol.* **2006**, *176*, 6665–6672. [[CrossRef](#)] [[PubMed](#)]
26. Nil, A.; Firat, E.; Sobek, V.; Eichmann, K.; Niedermann, G. Expression of Housekeeping and Immunoproteasome Subunit Genes Is Differentially Regulated in Positively and Negatively Selecting Thymic Stroma Subsets. *Eur. J. Immunol.* **2004**, *34*, 2681–2689. [[CrossRef](#)] [[PubMed](#)]
27. Murata, S.; Takahama, Y.; Kasahara, M.; Tanaka, K. The Immunoproteasome and Thymoproteasome: Functions, Evolution and Human Disease. *Nat. Immunol.* **2018**, *19*, 923–931. [[CrossRef](#)] [[PubMed](#)]
28. Ohigashi, I.; Matsuda-Lennikov, M.; Takahama, Y. Peptides for T Cell Selection in the Thymus. *Peptides* **2021**, *146*, 170671. [[CrossRef](#)]
29. Groettrup, M.; Soza, A.; Eggers, M.; Kuehn, L.; Dick, T.P.; Schild, H.; Rammensee, H.G.; Koszinowski, U.H.; Kloetzel, P.M. A Role for the Proteasome Regulator PA28 α in Antigen Presentation. *Nature* **1996**, *381*, 166–168. [[CrossRef](#)]
30. Schwarz, K.; Eggers, M.; Soza, A.; Koszinowski, U.H.; Kloetzel, P.M.; Groettrup, M. The Proteasome Regulator PA28 α/β Can Enhance Antigen Presentation without Affecting 20S Proteasome Subunit Composition. *Eur. J. Immunol.* **2000**, *30*, 3672–3679. [[CrossRef](#)]
31. Murata, S.; Udono, H.; Tanahashi, N.; Hamada, N.; Watanabe, K.; Adachi, K.; Yamano, T.; Yui, K.; Kobayashi, N.; Kasahara, M.; et al. Immunoproteasome Assembly and Antigen Presentation in Mice Lacking Both PA28 α and PA28 β . *EMBO J.* **2001**, *20*, 5898–5907. [[CrossRef](#)] [[PubMed](#)]
32. Schulz, M.; Aichele, P.; Vollenweider, M.; Bobe, F.W.; Cardinaux, F.; Hengartner, H.; Zinkernagel, R.M. Major Histocompatibility Complex—Dependent T Cell Epitopes of Lymphocytic Choriomeningitis Virus Nucleoprotein and Their Protective Capacity against Viral Disease. *Eur. J. Immunol.* **1989**, *19*, 1657–1667. [[CrossRef](#)] [[PubMed](#)]
33. Toes, R.E.M.; Nussbaum, A.K.; Degermann, S.; Schirle, M.; Emmerich, N.P.N.; Kraft, M.; Laplace, C.; Zwinderman, A.; Dick, T.P.; Müller, J.; et al. Discrete Cleavage Motifs of Constitutive and Immunoproteasomes Revealed by Quantitative Analysis of Cleavage Products. *J. Exp. Med.* **2001**, *194*, 1–12. [[CrossRef](#)] [[PubMed](#)]
34. Li, J.; Hu, S.; Johnson, H.W.B.; Kirk, C.J.; Xian, P.; Song, Y.; Li, Y.; Liu, N.; Groettrup, M.; Basler, M. Co-Inhibition of Immunoproteasome Subunits LMP2 and LMP7 Enables Prevention of Transplant Arteriosclerosis. *Cardiovasc. Res.* **2023**, *119*, 1030–1045. [[CrossRef](#)] [[PubMed](#)]
35. Basler, M.; Li, J.; Groettrup, M. On the Role of the Immunoproteasome in Transplant Rejection. *Immunogenetics* **2019**, *71*, 263–271. [[CrossRef](#)] [[PubMed](#)]
36. Vogelbacher, R.; Meister, S.; Gückel, E.; Starke, C.; Wittmann, S.; Stief, A.; Voll, R.; Daniel, C.; Hugo, C. Bortezomib and Sirolimus Inhibit the Chronic Active Antibody-Mediated Rejection in Experimental Renal Transplantation in the Rat. *Nephrol. Dial. Transplant* **2010**, *25*, 3764–3773. [[CrossRef](#)] [[PubMed](#)]
37. Buerger, S.; Herrmann, V.L.; Mundt, S.; Trautwein, N.; Groettrup, M.; Basler, M. The Ubiquitin-like Modifier FAT10 Is Selectively Expressed in Medullary Thymic Epithelial Cells and Modifies T Cell Selection. *J. Immunol.* **2015**, *195*, 4106–4116. [[CrossRef](#)] [[PubMed](#)]
38. Dick, T.P.; Ruppert, T.; Groettrup, M.; Kloetzel, P.M.; Kuehn, L.; Koszinowski, U.H.; Stevanovic, S.; Schild, H.; Rammensee, H.-G. Coordinated Dual Cleavages Induced by the Proteasome Regulator PA28 Lead to Dominant MHC Ligands. *Cell* **1996**, *86*, 253–262. [[CrossRef](#)] [[PubMed](#)]
39. Yamano, T.; Murata, S.; Shimbara, N.; Tanaka, N.; Chiba, T.; Tanaka, K.; Yui, K.; Udono, H. Two Distinct Pathways Mediated by PA28 and Hsp90 in Major Histocompatibility Complex Class I Antigen Processing. *J. Exp. Med.* **2002**, *196*, 185–196. [[CrossRef](#)]
40. Alfaro, E.; Díaz-García, E.; García-Tovar, S.; Zamarrón, E.; Mangas, A.; Galera, R.; López-Collazo, E.; García-Río, F.; Cubillos-Zapata, C. Upregulated Proteasome Subunits in COVID-19 Patients: A Link with Hypoxemia, Lymphopenia and Inflammation. *Biomolecules* **2022**, *12*, 442. [[CrossRef](#)]
41. Tian, G.; Li, M.; Lv, G. Analysis of T-Cell Receptor Repertoire in Transplantation: Fingerprint of T Cell-Mediated Alloresponse. *Front. Immunol.* **2022**, *12*, 778559. [[CrossRef](#)] [[PubMed](#)]
42. Son, E.T.; Faridi, P.; Paul-Heng, M.; Leong, M.L.; English, K.; Ramarathinam, S.H.; Braun, A.; Dudek, N.L.; Alexander, I.E.; Lisowski, L.; et al. The Self-Peptide Repertoire Plays a Critical Role in Transplant Tolerance Induction. *J. Clin. Investig.* **2021**, *131*, e146771. [[CrossRef](#)] [[PubMed](#)]
43. Tanahashi, N.; Murakami, Y.; Minami, Y.; Shimbara, N.; Hendil, K.B.; Tanaka, K. Hybrid Proteasomes. Induction by Interferon-Gamma and Contribution to ATP-Dependent Proteolysis. *J. Biol. Chem.* **2000**, *275*, 14336–14345. [[CrossRef](#)] [[PubMed](#)]
44. Zhou, J.; He, W.; Luo, G.; Wu, J. Fundamental Immunology of Skin Transplantation and Key Strategies for Tolerance Induction. *Arch. Immunol. Ther. Exp.* **2013**, *61*, 397–405. [[CrossRef](#)]

45. Fabre, B.; Lambour, T.; Delobel, J.; Amalric, F.; Monsarrat, B.; Burlet-Schiltz, O.; Bousquet-Dubouch, M.P. Subcellular Distribution and Dynamics of Active Proteasome Complexes Unraveled by a Workflow Combining in Vivo Complex Cross-Linking and Quantitative Proteomics. *Mol. Cell. Proteomics* **2013**, *12*, 687–699. [[CrossRef](#)] [[PubMed](#)]
46. Bitzer, A.; Basler, M.; Krappmann, D.; Groettrup, M. Immunoproteasome Subunit Deficiency Has No Influence on the Canonical Pathway of NF- κ B Activation. *Mol. Immunol.* **2017**, *83*, 147–153. [[CrossRef](#)] [[PubMed](#)]
47. Groettrup, M.; Ruppert, T.; Kuehn, L.; Seeger, M.; Standera, S.; Koszinowski, U.; Kloetzel, P.M. The Interferon- γ -Inducible 11 S Regulator (PA28) and the LMP2/LMP7 Subunits Govern the Peptide Production by the 20 S Proteasome in Vitro. *J. Biol. Chem.* **1995**, *270*, 23808–23815. [[CrossRef](#)] [[PubMed](#)]
48. Karttunen, J.; Sanderson, S.; Shastri, N. Detection of Rare Antigen-Presenting Cells by the LacZ T-Cell Activation Assay Suggests an Expression Cloning Strategy for T-Cell Antigens. *Proc. Natl. Acad. Sci. USA* **1992**, *89*, 6020–6024. [[CrossRef](#)] [[PubMed](#)]
49. Mundt, S.; Basler, M.; Sawitzki, B.; Groettrup, M. No Prolongation of Skin Allograft Survival by Immunoproteasome Inhibition in Mice. *Mol. Immunol.* **2017**, *88*, 32–37. [[CrossRef](#)]
50. Basler, M.; Lauer, C.; Beck, U.; Groettrup, M. The Proteasome Inhibitor Bortezomib Enhances the Susceptibility to Viral Infection. *J. Immunol.* **2009**, *183*, 6145–6150. [[CrossRef](#)]

Disclaimer/Publisher’s Note: The statements, opinions and data contained in all publications are solely those of the individual author(s) and contributor(s) and not of MDPI and/or the editor(s). MDPI and/or the editor(s) disclaim responsibility for any injury to people or property resulting from any ideas, methods, instructions or products referred to in the content.